Available online at www.sciencedirect.com
SCIENCE DIRECT®
Coordination Chemistry Reviews 249 (2005) 1310–1315
COORDINATION CHEMISTRY REVIEWS
www.elsevier.com/locate/ccr

Review

Photochemical reactions of rhodium(III) diimine complexes in solid glycerol matrices Ligand-field influences on activation parameters

J.A. Brozik [a], G.A. Crosby [b,*]

[a] *Department of Chemistry, University of New Mexico, Albuquerque, NM 87131, USA*
[b] *Department of Chemistry, Washington State University, Pullman, WA 99164-4630, USA*

Accepted 8 March 2005
Available online 4 June 2005

Contents

Abstract

At temperatures below 150 K in rigid glycerol glasses $[Rh(CN)_2(s\text{-}NN)_2]PF_6$ complexes display a $^3\pi\pi^* \rightarrow$ gs phosphorescence characteristic of the s-NN ligand [s-NN = 1,10-phenanthroline (phen), 4-Mephen, 4,7-Me_2phen, and 3,4,7,8-Me_4phen]. Above 150 K but below the melting point of glycerol a temperature-dependent first-order reaction occurs upon irradiation with UV light. The temperature dependences of these photochemical reactions conform to the Arrhenius equation with an activation energy range of 2000–2500 cm^{-1}, which is a range averaging 725 cm^{-1} lower than that previously reported for $[Rh(s\text{-}NN)_3](PF_6)_3$ complexes. These results are interpreted in terms of the thermal redistribution of energy from an unreactive $^3\pi\pi^*$ excited term to a close-lying chemically reactive ^{3}dd level that has been lowered in energy with respect to that of the corresponding $[Rh(s\text{-}NN)_3](PF_6)_3$ complex. The relationships of the Arrhenius activation energies to the electronic structures of the parent complexes and to the natures of the products are discussed.

Keywords: Rhodium(III) complexes; Photophysics; Photochemistry; Activation energies; Phosphorescence; Emission spectra; Lifetimes; Crystal field

* Corresponding author. Tel.: +1 509 448 3890; fax: +1 509 448 3890.
E-mail address: gac@wsunix.wsu.edu (G.A. Crosby).

0010-8545/$ – see front matter © 2005 Elsevier B.V. All rights reserved.
doi:10.1016/j.ccr.2005.03.020

1. Introduction

Photosubstitutional reactions of $[Rh(diimine)_3]^{3+}$ complexes (tris complexes) in solid glycerol glasses at temperatures above 150 K have been reported [1,2]. These reactions produce single photoproducts that have been tentatively identified as $[Rh(diimine)_2(diimine{:}H^+)(glyceroxide)]^{3+}$ species. The reaction rates were highly temperature-dependent and activation energies were determined. These activation energies were related to the gap between the lowest $^3\pi\pi^*$ level and a higher-lying chemically reactive ^{3}dd manifold. The initial investigation quantified the effect of tuning the lowest $^3\pi\pi^*$ level, through methyl substitution on the phen backbone, on the photochemical activation energy [2]. In the present contribution the strength of the crystal field around the central rhodium ion has been varied by ligand substitution. Specifically, one of the diimine ligands (tris complexes) has been replaced by two stronger field cyanide ligands (dicyano complexes). Activation energies of the dicyano complexes are then compared with those obtained from the corresponding tris complexes. Finally, the chemical and photophysical natures of the new photoproducts have been investigated.

2. Experimental

2.1. Syntheses

$[Rh(Cl)_2(s\text{-}NN)_2]Cl$ complexes were anaerobically prepared from $RhCl_3$ hydrate (2 mmol) and a slight excess of the diimine ligand (4.2 mmol) in a reaction vessel attached to a vacuum line. The reactants were degassed by maintaining them at a pressure below 1 mTorr for ∼12 h. A 75% aqueous ethanol solvent, rigorously degassed, was condensed on the reactant mixture. The resultant slurry was stirred under gentle warming and after ∼1 h a yellow-orange solution appeared. The solution was then allowed to evaporate to dryness, and the product was subsequently recrystallized from hot methanol. In all cases, well-formed bright yellow crystals of $[Rh(Cl)_2(s\text{-}NN)_2]Cl$ were obtained.

The $[Rh(CN)_2(s\text{-}NN)_2]PF_6$ complexes were prepared anaerobically from $[Rh(Cl)_2(s\text{-}NN)_2]Cl$ (1 mmol) and a twofold excess of NaCN (4 mmol) in a reaction vessel attached to a vacuum line. The solid reactants were degassed by maintaining them at a pressure below 1 mTorr for ∼12 h. Deionized water, carefully degassed by three consecutive freeze–pump–thaw cycles, was then condensed on the reactants. The mixture was stirred under gentle warming. Immediately, while still cold, the slurry turned from yellow to clear producing a white precipitate. Warming was continued until all the precipitate had dissolved and a colorless solution appeared. The solution was removed from the vacuum line and treated with concentrated HCl to remove excess CN^- as HCN gas. The solution was concentrated and cooled in an ice bath whereupon small crystals formed.

To effect purification, the crystals were collected and redissolved in warm water. The crude product was then loaded on a CM-Sephadex-C25 cation exchange column (12 in. × 1 in. i.d.), which had been equilibrated with deionized water. The column was interfaced with a Pharmacia UV detector and a stripchart recorder to monitor the emerging bands. The eluant was water followed by solutions of NaCl stepped from 0.1 to 0.5N. A very small colorless band came off with the mobile water phase. The largest band, containing the product, came off with the application of 0.1N NaCl. A very small dark impurity band was washed off the column during the 0.5N NaCl step. Hexafluorophosphate salts of the complexes were produced through metathesis of the chlorides with a concentrated, filtered, neutralized solution of $NaPF_6$. All complexes were obtained as white powders.

2.2. Sample preparation

Emission and lifetime measurements were performed on 10^{-4} M solutions in glycerol. Photochemical reaction rates were measured on 5×10^{-6} M solutions in rigorously degassed glycerol kept O_2 free with ambient N_2 gas. Photochemical reaction rate measurements were always conducted on fresh samples. For spectroscopic characterization photoproducts were generated through exhaustive photolysis of 10^{-4} M $[Rh(CN)_2(s\text{-}NN)_2]PF_6$ in glycerol glasses at 200 K. [The glycerol was vigorously degassed prior to use and samples were kept free of O_2.]

2.3. Spectroscopic measurements

Steady-state emission and lifetime measurements were conducted as described previously [2]. The excitation source was the 325-nm line of a 4-mW HeCd laser. The detection system was a thermoelectrically cooled Hamamatsu R943-02 PMT coupled to an SRS-400 photon counter. For decay-time measurements the excitation beam was modulated mechanically.

2.4. Measurement of activation energies

Photochemical reaction rates were obtained by measuring the rate of disappearance of the characteristic $^3\pi\pi^* \rightarrow$ gs phosphorescence of the parent $[Rh(CN)_2(s\text{-}NN)_2]PF_6$ complex. The band was monitored at the emission maximum. The optical setup and the fiber-optic sample rod constructed for measuring the photochemical reaction rates were described previously [2]. Activation energies were determined by fitting the photochemical rates to the Arrhenius equation:

$$\ln k_{obs} = -(\Delta\varepsilon/k)(1/T) + \ln A$$

where k_{obs} is the observed reaction rate, $\Delta\varepsilon$ the activation energy, and k the Boltzmann constant (in $cm^{-1}\,K^{-1}$).

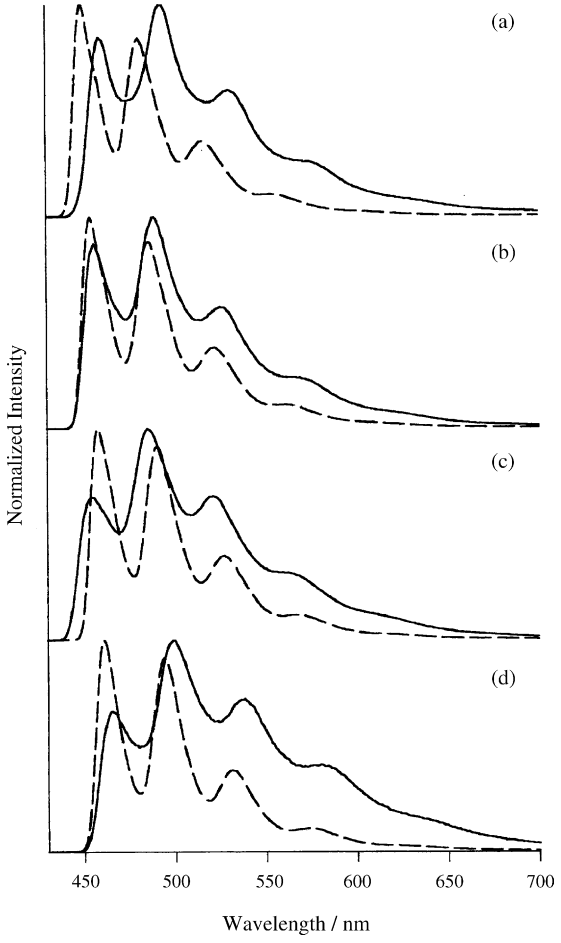

Fig. 1. Steady-state emission spectra at 77 K of $[Rh(CN)_2(s\text{-}NN)_2]PF_6$ complexes (- - -) and the corresponding photoproducts (—) in glycerol glasses at 10^{-4} M. Samples excited with a 325-nm HeCd laser line: (a) $[Rh(CN)_2(phen)_2]PF_6$, (b) $[Rh(CN)_2(4\text{-}Mephen)_2]PF_6$, (c) $[Rh(CN)_2(4,7\text{-}Me_2phen)_2]PF_6$, (d) $[Rh(CN)_2(3,4,7,8\text{-}Me_4phen)_2]PF_6$.

3. Results

3.1. Emission spectra

Displayed in Fig. 1 are the steady-state emission spectra of the $[Rh(CN)_2(s\text{-}NN)_2]PF_6$ complexes and their corresponding photoproducts. The spectra of the title complexes are typically structured $^3\pi\pi^* \rightarrow$ gs phosphorescences. The energies of the band maxima and the band profiles are similar to the phosphorescences observed from the corresponding free ligands and they are almost identical to those of the corresponding tris molecules [2]. The energies of the phosphorescence band maxima decrease in the order $[Rh(CN)_2(phen)_2]PF_6 > [Rh(CN)_2(4\text{-}Mephen)_2]PF_6 > [Rh(CN)_2(4,7\text{-}Me_2phen)_2]PF_6 > [Rh(CN)_2(3,4,7,8\text{-}Me_4phen)_2]PF_6$.

Steady-state UV irradiation of the photoproducts generates intense phosphorescences with band shapes and energies similar to those of the phosphorescences of the monoprotonated ligands and nearly identical to those of the corresponding $[Rh(s\text{-}NN)_3](PF_6)_3$ photoproducts [2]. Similar to the $[Rh(s\text{-}NN)_3](PF_6)_3$ photoproducts, but unlike the monoprotonated ligands, the photoproducts of the dicyano complexes emit no detectable fluorescence.

Table 1
Lifetimes of monoprotonated ligands, dicyano complexes, and photoproducts at 77 K

s-NN	s-NN:H^+[a]	$[Rh(CN)_2(s\text{-}NN)_2]PF_6$[a]	Photoproduct[a]
phen	1.873	55.1×10^{-3}	2.56×10^{-3}
4-Mephen	2.018	62.7×10^{-3}	3.19×10^{-3}
4,7-Me_2phen	1.783	72.5×10^{-3}	2.91×10^{-3}
3,4,7,8-Me_4phen	1.938	67.7×10^{-3}	2.57×10^{-3}

[a] All lifetimes in seconds.

3.2. Lifetimes

Phosphorescence decay curves of the $[Rh(CN)_2(s\text{-}NN)_2]PF_6$ complexes were fit to a single exponential over five lives with minimal residuals. Their lifetimes and those of the corresponding photoproducts are listed in Table 1. Phosphorescence decays of the title complexes ranged from 55.1 to 72.5 ms, a range that is slightly higher than that observed for the corresponding $[Rh(s\text{-}NN)_3](PF_6)_3$ series (40.6–48.6 ms) [2]. Phosphorescence decays of the $[Rh(CN)_2(s\text{-}NN)_2]PF_6$ photoproducts ranged from 2.6 to 3.2 ms, again a range slightly higher than that observed for the corresponding $[Rh(s\text{-}NN)_3](PF_6)_3$ photoproducts (2.0–2.8 ms) [2].

3.3. Activation energies

As reported for complexes of the type $[Rh(s\text{-}NN)_3](PF_6)_3$, the photochemical reactions of the $[Rh(CN)_2(s\text{-}NN)_2]PF_6$ species in solid glycerol glasses were also first order as inferred from the rigorously exponential decay of the phosphorescence intensity of each parent complex under constant illumination. As expected, the observed reaction rates were independent of concentration but directly proportional to excitation intensity. As shown in Fig. 2, the temperature dependence of this first-order reaction follows the Arrhenius equation yielding activation energies that range from 2000 to 2500 cm^{-1} (Table 2). On average the values are 725 cm^{-1} less than those obtained for the corresponding $[Rh(s\text{-}NN)_3](PF_6)_3$ complexes. Unlike the $[Rh(s\text{-}NN)_3](PF_6)_3$ complexes, however, which show only a rough correlation between activation energies and the $^3\pi\pi^*$ phosphorescence band maxima, the $[Rh(CN)_2(s\text{-}NN)_2]PF_6$ complexes display a *quantitative* cor-

Table 2
Summary of $^3\pi\pi^*$ energies and Arrhenius activation barriers

Complex	First $^3\pi\pi^* \rightarrow$ gs band max (cm^{-1})	Activation energies ($\pm 50\ cm^{-1}$)
$[Rh(CN)_2(phen)_2]PF_6$	22260	2000
$[Rh(CN)_2(4\text{-}Mephen)_2]PF_6$	22030	2200
$[Rh(CN)_2(4,7\text{-}Me_2phen)_2]PF_6$	21850	2400
$[Rh(CN)_2(3,4,7,8\text{-}Me_4phen)_2]PF_6$	21720	2500

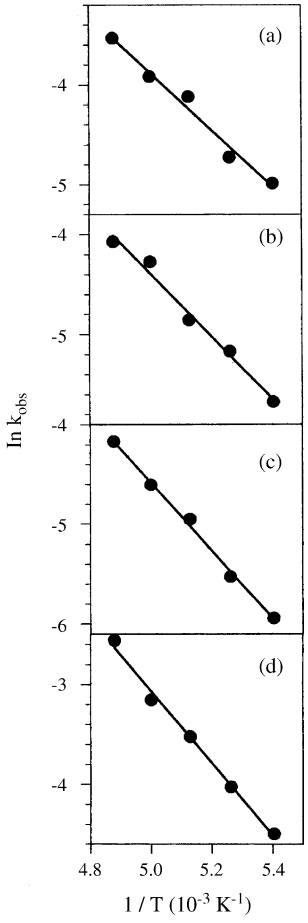

Fig. 2. Arrhenius plots for the photochemical reaction of $[Rh(CN)_2(s\text{-}NN)_2]PF_6$ complexes. Each point obtained from a fit to a single exponential over four natural lives: (a) $[Rh(CN)_2(phen)_2]PF_6$, (b) $[Rh(CN)_2(4\text{-}Mephen)_2]PF_6$, (c) $[Rh(CN)_2(4,7\text{-}Me_2phen)_2]PF_6$, (d) $[Rh(CN)_2(3,4,7,8\text{-}Me_4phen)_2]PF_6$.

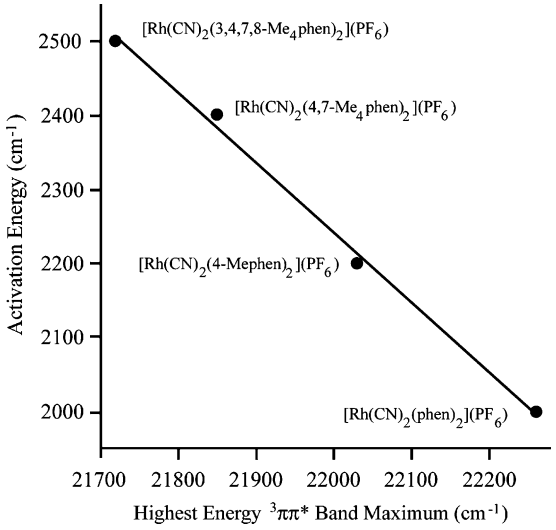

Fig. 3. Correlation between the phosphorescence band maxima and the measured activation energies for $[Rh(CN)_2(s\text{-}NN)_2]PF_6$ complexes.

relation within the experimental error of the measurements (see Fig. 3). Specifically, the energies of the band maxima are linearly related to the activation energies with a slope of ~ -1. Analogous to the results from the $[Rh(s\text{-}NN)_3](PF_6)_3$ series, the species with the highest energy phosphorescence band maximum has the lowest activation energy, whereas the complex with the lowest energy phosphorescence possesses the highest activation energy.

4. Discussion

4.1. Kinetic model

It is clear that the photoreactions of the dicyano complexes, $[Rh(CN)_2(s\text{-}NN)_2]PF_6$, proceed in the same manner as reported previously for the tris complexes, $[Rh(s\text{-}NN)_3](PF_6)_3$. Both series are structurally similar and have similar excited-state properties. Both sets of photoreactions follow characteristic first-order kinetics in solid glycerol matrices to produce spectroscopically similar photoproducts. The reaction rates for both series of molecules display temperature dependences that rigorously follow the Arrhenius relation.

As detailed for the tris complexes, the proposed scheme to account for the photochemistry of the dicyano complexes again invokes the participation of a photoactive ^{3}dd level. To generate this model we first assume that the metal–ligand bonding and the crystal (electrostatic) field strengths of all the diimine ligands are similar, thus placing the nearby-lying ^{3}dd level at approximately the same energy in every complex. Upon irradiation, energy from the lowest $^3\pi\pi^*$ level is thermally redistributed to a nearby chemically active ^{3}dd manifold that leads to a rapid photosubstitution reaction. Such a mechanism is consistent with the fact that the complex with the *highest* $^3\pi\pi^*$ energy possesses the *lowest* activation energy. This is also in concert with the nearly exact negative correlation observed between the highest energy $^3\pi\pi^*$ peak and the measured activation energy in each dicyano complex.

As already noted, there are two major differences between the sets of activation energies determined for the $[Rh(CN)_2(s\text{-}NN)_2]PF_6$ complexes and those for the $[Rh(s\text{-}NN)_3](PF_6)_3$ series. For corresponding s-phen ligands (a) the values for the dicyano complexes average $\sim$725 cm^{-1} lower in energy and (b) there is an exact negative correlation between the $^3\pi\pi^*$ band maxima and the measured activation energies for the dicyano species, whereas the values for the tris complexes displayed a rough correlation only. The first observation can be understood by simply analyzing the field around the central metal ion. If one considers only the microsymmetry around the Rh^{3+} ion, the tris complexes have nearly O_h microsymmetry whereas the dicyano complexes possess C_{2v} microsymmetry. Therefore, in the tris complexes, the d-orbitals are split into the well known t_{2g} and e_g sets. As shown in Fig. 4, upon replacement of one of the s-NN ligands with two cyanide anions three of the d-orbitals will be perturbed by the stronger field ligands, while two will remain essentially undisturbed.

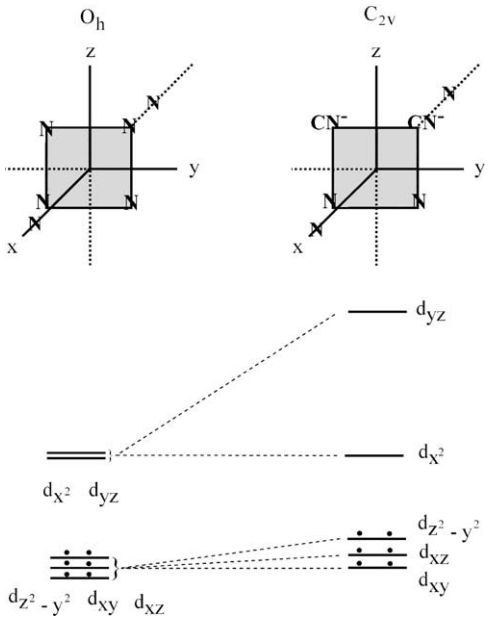

Fig. 4. The d-orbital correlation scheme for $[Rh(s\text{-}NN)_3](PF_6)_3$ under O_h microsymmetry and $[Rh(CN)_2(s\text{-}NN)_2]PF_6$ under C_{2v} microsymmetry. Labels are chosen to make *z* the principal axis in C_{2v}.

The unoccupied d_{yz} (e_g under O_h symmetry) orbital will be pushed up in energy the most because its lobes are directed toward the cyanide ligands; the d_{x^2} orbital will be basically unperturbed by the higher field ligands because its lobes are perpendicular to the plane containing the cyanides.

Of the occupied orbitals (t_{2g} in O_h), the $d_{z^2-y^2}$ will be affected the most because one of the lobes is directed between the CN^- ligands while the d_{xz} will only be slightly perturbed. The d_{xy} orbital should remain essentially undisturbed because it lies in a plane perpendicular to the plane containing the cyanide ligands. These simple crystal-field arguments lead to the prediction that the gap between the highest occupied and the lowest unoccupied d-orbital is somewhat smaller for the dicyano complexes than for the tris complexes. Consequently the ^{3}dd manifold should lie lower in energy in the dicyano series, thus placing it closer to the $^3\pi\pi^*$ level of the heterocyclic ligand than in the tris series. Accordingly, the narrowing of the ^{3}dd–$^3\pi\pi^*$ gap should cause the dicyano complexes to have lower activation energies than the corresponding tris species. As noted above, the average of the measured activation energies for the dicyano complexes is $\sim$725 cm^{-1} lower than that of the tris series lending even greater credence to the proposed photochemical pathway.

We emphasize that the rationalization of the lowering of the photochemical activation energies of the dicyano complexes relative to their parent tris molecules rests on purely electrostatic (crystal) field arguments based on the lowering of the microsymmetry about the metal ion by the introduction of the cyanide ions into the coordination sphere. Since the two cyanides provide a stronger field than a single diimine, the effect of the reduction in microsymmetry on the orbital energies is necessary to account for the experimental results. A simple average (octahedral) field model will not suffice. To account for the experimental results quantitatively, a model that takes into account the reduction in total charge of the species and the effects of covalency would be required.

Finally, we address the observation that the tris complexes show only a rough negative correlation between the $^3\pi\pi^*$ $\rightarrow$ gs band maxima and the measured activation energies, whereas the dicyano complexes display an exact negative linear correlation. In open (sterically unhindered) complexes of the type $[RhCl_2(diimine)_2]Cl$ and $K[RhCl_4(diimine)]$, which are known ^{3}dd $\rightarrow$ gs emitters, it has been shown that methyl substitution of the 1,10-phenanthroline or 2,2′-bipyridine backbone has little or no effect on the observed emission energies [3–5]. Thus the ligand field around the Rh^{3+} ion appears to be unchanged upon methyl substitution. The bands are broad, however, and the energy measured lacks precision. Because the dicyano complexes display an exact negative correlation (slope = −1) between measured activation energies and $^3\pi\pi^*$ $\rightarrow$ gs emission maxima, we infer that this insensitivity [of methyl substitution on the ligand field] also holds within this series of rhodium(III) complexes. In contrast, the tris complexes display only a rough negative correlation with deviations from linearity of $\pm$500 cm^{-1}. We conjecture that such deviations are due to steric interactions in the crowded tris complexes that are not present in the more open dicyano structures.

Steric effects have been reported for other crowded Rh(III) and Ru(II) complexes, namely $[Rh(dmbpy)_3](ClO_4)_3$ and $[Ru(pq)_3](ClO_4)_2$ [4,6], which exhibit a lowering of a close-lying ^{3}dd manifold presumably caused by steric crowding. It is reasonable to expect that the same type of steric interaction may also be present in the $[Rh(s\text{-}NN)_3](PF_6)_3$ complexes, albeit to a much lesser extent. The net result would be to lower the ^{3}dd manifold closer to the lowest $^3\pi\pi^*$ level, slightly decreasing the measured activation energies from the values expected for unhindered species. Whereas two of the four tris complexes possess activation energies slightly lower than those expected from a presumed linear correlation, $[Rh(3,4,7,8\text{-}Me_4phen)_3](PF_6)_3$ has an activation energy slightly higher than expected. To account for this, it is reasonable to suggest that steric crowding not only affects the ligand field around the central metal ion but also modifies the measured activation energy by creating a Franck–Condon barrier to photochemical substitution.

4.2. Nature of the photoproduct

The proposed photochemical reaction for $[Rh(CN)_2(phen)_2]PF_6$ is depicted below. Ion exchange chromatography has revealed ionic properties of the photoproduct identical to those of the original parent complex; upon elution through a CM-Sephadex-C25 column (12 in. × 1 in. i.d.) both the product and starting complex came off with identical amounts of 0.1N NaCl, thus indicating that no redox chemistry had occurred. Moreover, because of the structural, photochemical, and spectroscopic similarities of the dicyano

parent complexes with those of the corresponding parent tris complexes and also the spectroscopic similarities of the resultant photoproducts, the photochemical reaction involving the dicyano complexes and the solid glycerol matrix is also presumed to be substitutional in nature. Thus, we tentatively identify the dicyano photoproducts as $[Rh(CN)_2(s\text{-}NN)(s\text{-}NN{:}H^+)(glyceroxide)]PF_6$:

$$[Rh(CN)_2(s\text{-}NN)_2]PF_6 + C_3H_5(OH)_3 \xrightarrow[T>150\,K]{h\nu} [Rh(CN)_2(s\text{-}NN)(s\text{-}NN : H^+)C_3H_5(OH)_2O^-]PF_6$$

Since the phosphorescence of each photoproduct is nearly identical to that of the corresponding monoprotonated uncomplexed ligand and also to that of the corresponding tris photoproduct, the luminescences from the dicyano photoproducts are assigned to $^3\pi\pi^* \rightarrow$ gs phosphorescences localized on the monodentate monoprotonated ligand. The measured transient decays (all on the order of 2 ms) are consistent with this assignment, because such lifetimes are expected for spin-orbit perturbed spin-forbidden transitions between states of primarily ligand orbital parentages [7].

Acknowledgment

Research was supported by a grant from the U.S. Department of Energy.

References

[1] J.A. Brozik, G.A. Crosby, Chem. Phys. Lett. 255 (1996) 445.
[2] J.A. Brozik, G.A. Crosby, J. Phys. Chem. 102 (1998) 45.
[3] D.H.W. Carstens, G.A. Crosby, J. Mol. Spectrosc. 34 (1970) 113.
[4] M. Nishizawa, T.M. Suzuki, S. Sprouse, R.J. Watts, P.C. Ford, Inorg. Chem. 23 (1984) 1837.
[5] J. Van Houten, R.J. Watts, J. Am. Chem. Soc. 96 (1974) 4334.
[6] D.M. Klassen, Inorg. Chem. 15 (1976) 3166.
[7] D.H.W. Carstens, R.J. Watts, G.A. Crosby, Science 170 (1970) 1195.